

# Fabrication of 2-Chloropyridine-Functionalized Fe<sub>3</sub>O<sub>4</sub>/Amino-Silane Core-Shell Nanoparticles

M.M.A. Nikje\*, L. Sarchami and L. Rahmani

Department of Chemistry, Faculty of Science, Imam Khomeini International University, Qazvin, I.R.Iran

(\* Corresponding author: Drmm.alavi@gmail.com

(Received: 27 Sep 2014 and Accepted: 22 Feb. 2015)

## Abstract:

In this report, magnetic iron oxide nanoparticles were synthesized via coprecipitation of Fe<sup>2+</sup> and Fe<sup>3+</sup> with ammonium hydroxide, and the surface of synthesized nanoparticles was organically functionalized by commercially available amine coupling agent namely, 3-aminopropyl trimethoxysilane (APTS) by using well-known sol-gel method. Further reaction of the synthesized Fe<sub>3</sub>O<sub>4</sub>@APTS core-shell magnetite nanoparticles with 2-Chloropyridine via nucleophilic aromatic mechanism in position 2 led to the target molecule Fe<sub>3</sub>O<sub>4</sub>@APTS/ 2-Chloropyridine. All prepared materials e.g the magnetite iron oxide, Fe<sub>3</sub>O<sub>4</sub>@APTS nanoparticles as well as organically coated Fe<sub>3</sub>O<sub>4</sub>@APTS/ 2-Chloropyridine magnetite particles were characterized using Fourier transforms infrared spectroscopy (FT-IR), scanning electron microscopy (SEM), and thermogravimetric analysis (TGA). SEM images showed that the Fe<sub>3</sub>O<sub>4</sub>@APTS/ 2-Chloropyridine nanoparticles were roughly spherical with average size of 45-55 nm. FTIR indicated the formation of a layer of APTS-Py on the surface of the Fe<sub>3</sub>O<sub>4</sub> magnetite core. Thermogravimetric analysis of the coated APTS-Py on the Fe<sub>3</sub>O<sub>4</sub> surface revealed that 8 % of organic materials coated on iron oxide nanoparticles.

**Keywords:** Magnetite nanoparticle, APTS coating, 2-Chloropyridine modification, Sol-gel method.

## 1. INTRODUCTION

Nanotechnology is a novel stage of knowledge and technical development with possible applications in different regions such as electronics, mechanics, metallurgical engineering and chemistry [1]. Nanometer-sized particles (NPs) have been quickly and widely developed [2]. Among different kinds of NPs, iron oxide magnetic nanoparticles have been gaining considerable attentions because of their exclusive magnetic properties.

Recently, magnetic nanoparticle (MNP) has become key constituents in various regions like bio separation in life-science [3]. Biomedicine and bioengineering such as the magnetically assisted drug delivery [4], biomacromolecule purification [5], label for

bio-separation [6,7], sensitive component for biosensing [8,9], contrast agent for MRI (magnetic resonance imaging) [10,11] and also as a nanosource of heat for magnetically induced cancer hyperthermia [12,13].

MNPs intended for biomedical applications are generally biocompatible ferrite powders coated with organic molecular shell able to confine active pharmaceutical agents grafting on the functionalized surface of magnetic NPs. Fe<sub>3</sub>O<sub>4</sub> are even stable against oxidation and exhibition remarkable magnetization, being chosen in numerous applications due also to their lack of toxicity [14-16].

Usually, surface of magnetite nanoparticle has been coated by an inert silica layer because surface of magnetite has a strong attraction towards silica and inhibits their aggregation in liquid and increases the chemical stability [17].

By proper coating, dipolar attraction between magnetic nanoparticles can be decreased [18]. In addition, high density of surface functional group of  $-NH_2$  on the silica layer allowing for connecting to other functional groups [19]. The aminosilane agent of 3-aminopropyl triethoxysilane (APTS) was considered a candidate for modification on the surface of  $Fe_3O_4$  NPs [20].

Pyridine was first isolated and characterized from bone oil and from coal tar by Anderson in 1846 [21]. In both biological and chemical systems, it plays a main role catalyzing. It has a lot of biological activities those including antiviral, anticancer, antidote, antileishmanial, antioxidant and antihepatic, antithrombin, antitubercular, etc [22]. In this paper, 2-Chloropyridine was selected for connecting to the active functional group on the silica layer coupled on MNPs because of high reactivity and all advantages that mentioned above.

Easily recoverable and reusable in the heterogeneous catalyst are two important discussable topics. A prominent characterize of supported MNPs catalyst is that they can be eagerly separated using an external magnet, which performs a simple separation of catalyst without filtration [23]. Here we focus on developing functionalized iron oxide nanoparticles with 3-aminopropyl trimethoxysilane (APTS) which has an active group of  $-NH_2$  connected to 2-Chloropyridine.

## 2. EXPERIMENTAL

### 2.1. Materials

Iron (II) chloride tetrahydrate ( $FeCl_2 \cdot 4H_2O$ , 99.7%), iron (III) chloride hexahydrate ( $FeCl_3 \cdot 6H_2O$ , 99.0%), ammonia ( $NH_3 \cdot H_2O$ , 25%–28%), ethanol ( $C_2H_5OH$  99.7%), 3-aminopropyl-trimethoxysilane (APTS), 2-Chloropyridine,  $CH_3CN$  and citric acid, were purchased from Merck and were used as received without further purification.

### 2.2. Instruments

The morphology and particle size of the magnetite,  $Fe_3O_4$ ,  $Fe_3O_4@APTS-Py$  were

perused by scanning electron microscopy (SEM). FT-IR spectra was done by Bruker Tensor 27 spectrophotometer. The TGA of  $Fe_3O_4$ ,  $Fe_3O_4@APTS-Py$  was performed with Perkin-Elmer Pyris Diamond TG under air atmosphere at a heating rate of 7.5 °C/min.

### 2.3. Preparation of $Fe_3O_4@APTS$ nanoparticles

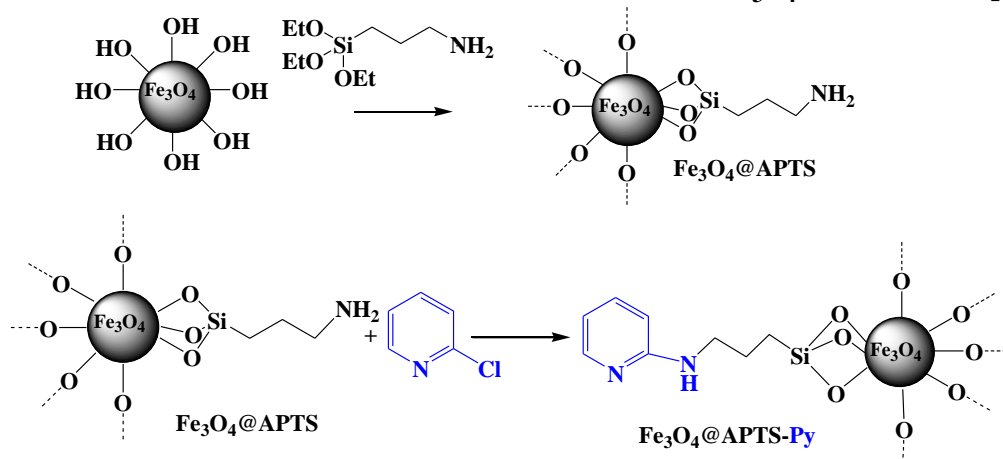
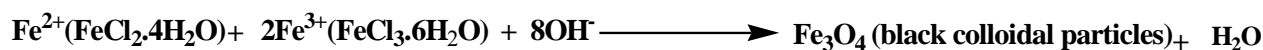
The MNPs were prepared through coprecipitation technique by the reaction of  $Fe^{3+}$  and  $Fe^{2+}$  (2/1 in mol/mol) precursors in agreement with prior reports [24]. For the synthesis of  $Fe_3O_4@APTS$  in the first step, magnetite nanoparticle (500 mg) was dispersed in 600-ml ethanol/water (5/1) and sonicated for 20 min. After acetic acid was added drop wise until pH set adjusted at 4. At that moment 4 ml APTS was added to the solution, and the mixture was stirred mechanically at room temperature for 3h. Lastly, the nanoparticle was separated and washed with distilled water for four times and after that dried at 45 °C in oven for 24 hours and characterized by FT-IR spectra [25].

### 2.4. Preparation of $Fe_3O_4@APTS-Py$ nanoparticles

The assembled  $Fe_3O_4@APTS$  nanoparticles were added to 10 mL of a saturated solution of 2-Chloropyridine in  $CH_3CN$ . The resulting mixture was stirred mechanically at 40°C for 12 hours. The material was obtained by magnetic separation followed by two times washing with 30 mL of  $CH_3CN$  consecutive before being dried at 45°C for 12 hours.

## 3. RESULTS AND DISCUSSION

Scheme 1 depicting the synthesis of  $Fe_3O_4@APTS-Py$ . The silane coating surface of the magnetic  $Fe_3O_4$  cores derived from the hydrolysis of APTS functioned as a coupling agent and provided amino group ( $-NH_2$ ) for binding the 2-Chloropyridine molecule. The characterization of nanoparticles were carried out by FTIR, TGA, SEM and VSM methods.



*Scheme 1. Reaction between  $\text{Fe}_3\text{O}_4$  with APTS,  $\text{Fe}_3\text{O}_4@APTS$  with 2-Chloropyridine*

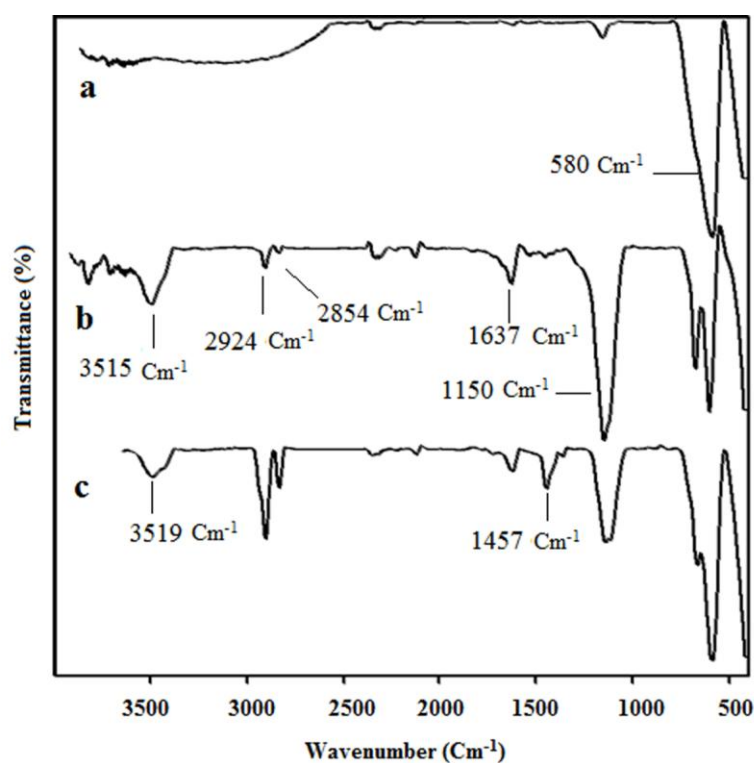


*Figure 1. FT-IR spectra of a  $\text{Fe}_3\text{O}_4$ , b  $\text{Fe}_3\text{O}_4@APTS$  and c  $\text{Fe}_3\text{O}_4@APTS\text{-Py}$  nanoparticles*

Figure 1 shows the Fourier transforms infrared (FTIR) spectra of (a)  $\text{Fe}_3\text{O}_4$ , (b)  $\text{Fe}_3\text{O}_4@APTS$ , and (c)  $\text{Fe}_3\text{O}_4@APTS$  modified by 2-Chloropyridine. In Figure 1 (a), the broad band in the range  $3400\text{-}3600 \text{ cm}^{-1}$  is due to the stretching vibrations of  $-\text{OH}$ , which is also appointed to the  $\text{OH}^-$  absorbed by  $\text{Fe}_3\text{O}_4$  nanoparticles. Strong peaks at about  $400 \text{ cm}^{-1}$  and  $580 \text{ cm}^{-1}$  are because of the stretching vibrations of Fe-O bond of magnetite nanoparticles.

In the spectrum for the modified nanoparticles, additional stretches are attributed to the presence of the organic layer on the surface of  $\text{Fe}_3\text{O}_4$  nanoparticles. In curve (b) and (c) two absorption peaks at  $2924$  and  $2854 \text{ cm}^{-1}$  are related to stretching vibration of C-H groups on APTS. Furthermore, in Figure 1 curve (b) and (c), the absorption band at  $1150 \text{ cm}^{-1}$  is attributed to Si-O-Si stretching vibration. Additionally, the absorption bands near  $3515 \text{ cm}^{-1}$  and  $1637 \text{ cm}^{-1}$  appear due to the

vibration of remainder H<sub>2</sub>O in the sample (b), and there also exists the contribution of –NH for the band near 3515 cm<sup>-1</sup>. In the meantime, the Fe-O-Si bonds cannot be seen in the FTIR spectrum of (b) and (c) since it appears at around 584 cm<sup>-1</sup> and accordingly overlaps with the Fe–O band of the Fe<sub>3</sub>O<sub>4</sub> [26-27]. In curve (c) the peak at 1457 cm<sup>-1</sup> is assigned to C=C band of Pyridine in (APTS-Py), and peak in 3519 cm<sup>-1</sup> is related to NH band.

The APTS-Py coating on the surface of Fe<sub>3</sub>O<sub>4</sub> NPs was also confirmed by TGA analysis. Figure 2 shows the TGA curves, portraying the variations of the residual masses of the samples with temperature. At high temperatures, the organic materials and magnetite of the samples are entirely burned to generate gas products and converted to iron oxides, respectively. The residual mass percentages estimated the magnetite amounts of the samples. As shown in Figure 2, TGA

chart of Fe<sub>3</sub>O<sub>4</sub>@APTS-Py nanoparticles indicated that the magnetite contents is about 92%. There is insignificant weight loss stage (below 130 °C) that can be imputed to the evaporation of water and ethanol molecules in sample (a), while in modified sample, weight loss started at 200 to 800°C and correspond to the thermal decomposition of  $\gamma$ -pyridyl-aminopropyl triethoxysilane (APTS-Py) coating on magnetite nanoparticles. Actually weight loss, the coated APTS-Py on the surface Fe<sub>3</sub>O<sub>4</sub> NPs is calculated as 8%.

To determine the average size and the morphology of Fe<sub>3</sub>O<sub>4</sub> and Fe<sub>3</sub>O<sub>4</sub>@APTS-Py nanoparticles scanning electron microscopy (SEM) was employed. In Figure 3, the SEM image of the Fe<sub>3</sub>O<sub>4</sub> (a) and Fe<sub>3</sub>O<sub>4</sub>@APTS-Py (b) shows that these particles were roughly spherical in shape, and the average size is about 30-40 and 45-55nm, respectively.

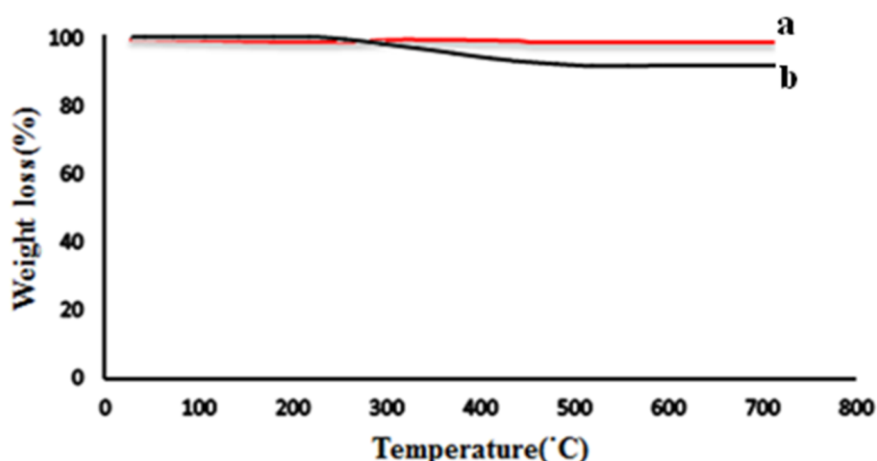


Figure 2. TGA curves for (a) Fe<sub>3</sub>O<sub>4</sub> and (b) Fe<sub>3</sub>O<sub>4</sub>@APTS-Py nanoparticles

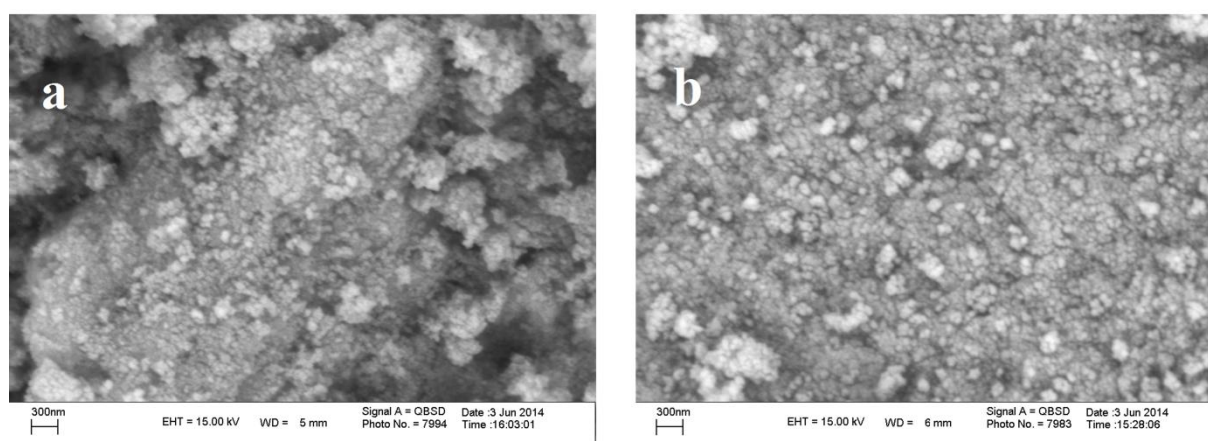
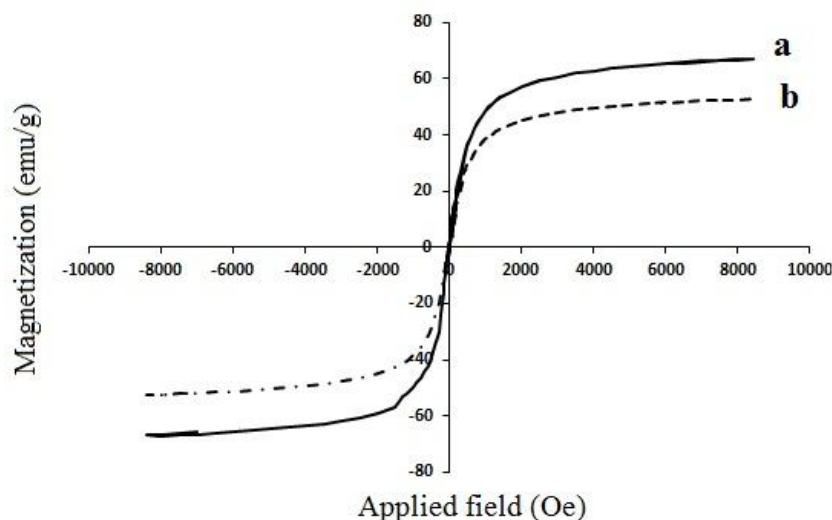


Figure 3. SEM images of synthesized a Fe<sub>3</sub>O<sub>4</sub> and b Fe<sub>3</sub>O<sub>4</sub>@APTS-Py nanoparticles



**Figure 4.** Magnetization hysteresis loops of a  $Fe_3O_4$  and b  $Fe_3O_4@APTS-Py$  nanoparticles

VSM was performed to investigate the magnetic properties of magnetite NPs ( $Fe_3O_4$ ) and magnetite NPs modified with APTS-Py. In figure 4 the saturation magnetization ( $M_s$ ) of  $Fe_3O_4$   $Fe_3O_4@APTS-Py$  is obtained 67 and 52 emu/g, respectively, where in  $M_s$  reduction corresponds to shell thickness. In addition, nanoparticles were shown superparamagnetic behavior at room temperature because no remanence magnetization is observed.

#### 4. CONCLUSIONS

As a result, by co-precipitation of ferrous and ferric salts nanosized  $Fe_3O_4$  particles were synthesized. Then, APTS-MNPs were prepared. Consequently, we coupled the 2-Chloropyridine with the APTS-MNPs through the substitution reaction at the C-2 position of 2-Chloropyridine by the  $-NH_2$ . The processes were monitored with SEM, FTIR, TGA and VSM.

SEM image showed that these nanoparticles were roughly spherical in shape with average size of 45-55 nm. FTIR indicated the formation of a layer of APTS-Py on the surface of the  $Fe_3O_4$  magnetite core. And by thermogravimetric analysis the coated Py-APTS on the  $Fe_3O_4$  surface is calculated as 8%.

#### REFERENCES

1. Huczko: Appl. Phys. A, vol. 70, No. 4, (2000), pp. 365-376.
2. L. Xie, R. Jiang, F. Zhu, H. Liu and G. Ouyang: Anal. Bioanal. Chem., Vol. 406, No. 2, (2014), pp. 377-399.
3. A. del Campo, T. Sen, J. P. Lellouche and I. J. Bruce: J. Magn. Magn. Mater., Vol. 293, No. 1, (2005), pp. 33-40.
4. S.C. Mc Bain, H.H. Yiu and J. Dobson: Int. J. Nanomedicine, Vol. 3, No. 2, (2008), pp. 169-180.
5. A. Elaissari, M. Rodrigue, F. Meunier and C. Herve: J. Magn. Magn. Mater., Vol. 225, No. 1-2, (2001), pp. 127-133.
6. Tibbe, B. de Grooth, J. Greve, P.A. Liberti, G. Dolan and L. Terstappen: Nat. Biotechnol., Vol. 17, No. 12, (1999), pp. 1210-1213.
7. P.A. Liberti, C.G. Rao and L.W. M.M. Terstappen: J. Magn. Magn. Mater., Vol. 225, No. 1, (2001), pp. 301-307.
8. Y.R. Chemla, H.L. Grossman, Y. Poon, R. Mc Dermott, R. Stevens, M.D. Alper and J. Clarke: Proc. Natl. Acad. Sci., Vol. 97, No. 26, (2000), pp. 14268-14272.
9. S.H. Chung, A. Hoffman, S.D. Bader, C. Liu, B. Kay and L. Chen: Appl. Phys. Lett., Vol. 85, No. 14, (2004), pp. 2971-2973.
10. J.W. Bulte, D.L. Kraitchman: NMR Biomed., Vol. 17, No. 7, (2004), pp. 484-489.
11. Zhang, M. Jugold, E. Woenne, T. Lammers, B. Morgenstern, M.M. Mueller, H. Zentgraf, M. Bock, M. Eisenhut, W. Semmler and F.

- Kiessling: *Cancer Res.*, Vol. 67, No. 4, (2007), pp. 1555-1562.
12. Jordan, R. Scholz, P. Wust, H. Fahlring and R. Felix: *J. Magn. Magn. Mater.*, Vol. 201, No. 1-3, (1999), pp. 413-419.
  13. Jordan, R. Scholz, P. Wust, H. Schirra, T. Schiestel, H. Schmidt and R. Felix: *J. Magn. Magn. Mater.*, Vol. 194, No. 1-3, (1999), pp. 185-196.
  14. S. Gustafsson, A. Fornara, K. Petersson, C. Johansson, M. Muhammed and E. Olsson: *Cryst. Growth Des.*, Vol. 10, No. 5, (2010), pp. 2278–2284.
  15. J.E. Kipp: *Int. J. Pharm.*, Vol. 248, No. 1-2, (2004), pp. 109-22.
  16. F.A. Tourinho, J. Depeyrot, G.J. da Silva and M.C.L. Lara: *Braz. J. Phys.*, Vol. 28, No. 4, (1998), pp. 413-427.
  17. Y. Sun, L. Duan, Z. Guo, Y. Duan Mu, M. Ma, L. Xu, Y. Zhang and N. Gu: *J. Magn. Magn. Mater.*, Vol. 285, No. 1-2, (2005), pp. 65-70.
  18. Y.S. Li, J.S. Church, A.L. Woodhead and F. Moussa: *Spectrochim Acta A.*, Vol. 76, No. 5, (2010), pp. 484-489.
  19. Y.H. Deng, C.C. Wang, J.H. Hu, W.L. Yang and S.K. Fu: *Colloids and Surfaces A: Physicochem. Eng. Aspects.*, Vol. 262, No. 1-3, (2005), pp. 87–93.
  20. X.C. Shen, X.Z. Fang, Y.H. Zhou and H. Liang: *Chem. Lett.*, Vol. 33, No. 11, (2004), pp. 1468-1469.
  21. Y. Higasio and T. Shoji: *Appl. Catal A-Gen.*, Vol. 221, No. 1-2, (2001), pp. 197-207.
  22. A. Chaubey and S.N. Pandeya: *Ajpcr.*, Vol. 4, No. 4, (2011), pp. 5-8.
  23. Girija, H.S. Bhojya Naik, B. Vinay Kumar and C.N. Sudhamani: *Am. Chem. Sci. J.*, Vol. 1, No.3, (2011), pp. 97-108.
  24. S. Wu, A. Sun, F. Zhai, J. Wang, W. Xu, Q. Zhang and A.A. Volinsky: *mater. Lett.*, Vol. 65, No. 12, (2011), pp. 1882-1884.
  25. M.M. Alavi Nikje, S. Tamaddoni Moghaddam, M. Noruzian, M. Farahmand Nejad, K. Shabani, M. Haghshenas and S. Shakhesi: *Colloid. Polym. Sci.*, Vol. 292, No. 3, (2014), pp. 627-633.
  26. H. Cao, J. He, L. Deng and X. Gao: *Appl. Surf. Sci.*, Vol. 255, No. 18, (2009), pp. 7974–7980.
  27. M. Ma, Y. Zhang, W. Yu, H.Y. Shen, H.Q. Zhang and N. Gu: *Colloid. Surface. A.*, Vol. 212, No. 2-3, (2003), pp. 219–226.